

MICROSTRUCTURAL ANALYSIS OF SOLAR CELL WELDS

T.J. Moore, G.K. Watson, and C.R. Baraona
NASA Lewis Research Center
Cleveland, Ohio

SUMMARY

Parallel-gap resistance welding of silicon solar cells with copper interconnects results in complex microstructural variations that depend on the welding variables. At relatively low heat input solid-state welds are produced. At medium heat the Ag-Cu eutectic forms resulting in a braze joint. High heat produces a fusion weld with complete melting of the silver layer on the silicon-solar cell. If the silicon is also melted, cracking occurs in the silicon cell below the weld nugget. These determinations were made using light microscopy, microprobe, and scanning electron microscopy analyses.

INTRODUCTION

Parallel-gap resistance welding (PGRW) has been used extensively in the production welding of interconnects to solar cells for space-power applications. Despite the fact that thousands of welds have been made, little information has been published on the microstructure of solar-cell welds. This investigation, though limited in scope, is an attempt to characterize the various microstructures that can be obtained when welding 39- μm (1.5-mil) thick copper interconnects to 200- μm (8-mil) thick silicon solar cells by PGRW. Solar-cell welds, made using three different weld schedules, were examined by optical and scanning electron microscopies. Compositional traces were obtained with an electron probe microanalyzer.

American Welding Society (AWS) terms and definitions are used throughout this report to make the technical discussions as clear as possible. The AWS Joint Method Diagram (fig. 1) is based on the physical state of the materials at the weld interface during coalescence (ref. 1). Thus, three metallurgical classifications of welding processes are defined:

- Fusion welding for liquid/liquid reaction
- Solid-state welding for solid/solid reaction
- Brazing and soldering for liquid/solid reaction

The authors are grateful to Frank M. Terepka, who performed the electron probe analysis.

MATERIALS

Cross sectional sketches of the silicon solar cell used in this study are shown in figure 2. These cells had 2-ohm cm, P-type base resistivity, shallow

junctions and wraparound insulator type contacts. At the P contact areas, four layers of material were deposited on the silicon (Si) cell:

- (1) Aluminum (Al) about 2000 Å thick
- (2) Titanium (Ti) about 1000 Å thick
- (3) Palladium (Pd) about 250 Å thick
- (4) Silver (Ag), 9 μm thick (7 to 13 μm by metallography)

The outer layer of silver was applied for electrical conductivity. The wraparound N-type contacts had the same silver, palladium, and titanium metal layers as the P contacts. However, instead of aluminum, the first layer deposited on the silicon cell was silicon dioxide (SiO₂) dielectric about 1 μm thick. This SiO₂ layer provided electrical insulation between the N-type contacts and the P-type silicon base layer.

The copper interconnect tab was cold-rolled stock with an average thickness of 39 μm. Metallographic examination showed a thickness variation of 37 to 46 μm.

PROCEDURE

Welding Equipment

Parallel-gap resistance welding is a variation of series resistance welding in which the electrodes are placed very close together. This electrode placement tends to produce relatively high heating and formation of a fusion weld nugget between the electrode. However, by controlled adjustment of the welding variables, it is possible to produce individual solid-state welds under each electrode.

In the welding head, an assembly with two molybdenum electrodes is used. Each side is electrically insulated from the other. Both electrodes move downward together on activation of their common supporting arm. Each electrode is permitted a controlled degree of flexing, which compensates for minor irregularities in flatness or thickness. This is important because good mechanical fit insures proper electrical contact between the electrodes and the work.

A constant-voltage power supply is used to produce a dynamically controlled single pulse of welding current. Welding is accomplished at a constant, preset voltage. Initiation of the welding power is automatic when a predetermined force is applied to the work by the electrodes.

Welding Schedules

Three weld schedules were applied in welding the copper interconnects to the silicon cells. Weld voltage is a primary variable because of the direct proportionality with welding current. Heat is generated in all portions of the circuit according to the formula:

$$H = I^2Rt$$

where H is the heat in joules, I is the current in amperes, R is the resistance in ohms, and t is the time of current flow in seconds. Welding time was

the second variable in this program (table I). Electrode force, which controls interfacial resistance, and the gap between the electrodes were held constant. Thus, the three weld schedules can be described as follows:

- Schedule A: Low heat for a long time
- Schedule B: Moderate heat for an intermediate time
- Schedule C: High heat for a short time

Welds were made with the same schedules for both the P and N contact areas in the solar cells.

Weld Examination

The solar-cell welds were mounted in clear epoxy for sectioning and metallographic polishing. Cross sections of the welds were examined at various locations along the electrode footprint denoted by section A-A in figure 3. Specific examples shown in this report were at positions 30 percent and 40 percent through the joints. A flat was polished on the side of the cylindrical metallographic mounts so that the weld footprint could be clearly seen. The specific location of the weld cross section after metallographic polishing could then be measured optically.

All of the weld cross sections were polished using standard metallographic techniques. The cross sections were examined optically up to 1000x. Although the welds were examined in both the unetched and etched conditions, all of the photomicrographs shown are in the unetched condition.

Selected samples were examined using a scanning electron microscope (SEM). Various areas of the samples were qualitatively analyzed using energy dispersive spectroscopy (EDS). In addition, an electron probe microanalyzer was used to obtain quantitative elemental distribution along continuous-line traverses through the weld regions.

RESULTS AND DISCUSSION

In the results to follow, an overview showing the electrode positions and the kinds of welds that were obtained with the various weld schedules will first be shown at 100x magnification. Higher magnification light photomicrographs with corresponding microprobe chemical analyses of the various weld joints will then be presented and discussed. The SEM was used to further examine braze areas, the solid-state weld interface and the SiO₂ layer at N contact area of the cells.

Schedule A Welds

The N contact weld shown in figure 4 (40 percent through the joint, table I) is a combination of solid-state welding and brazing. The SEM photomicrograph in figure 5 shows that dendrites in the braze metal are oriented normal to the braze interface, which is parallel to the expected direction of solidification. This shows that Cu interconnects can be joined to the Ag layer on the cell by resistance brazing rather than by conventional fusion resistance welding.

Ag-Cu solid-state welded areas (fig. 4) were present towards the outsides of the electrode footprints beyond the brazed regions.

Solid-state welding is achieved instantaneously when the resistance heated Ag and Cu surfaces are brought into intimate contact. Welding occurs at about $0.8 T_m$ of Ag (710°C), where T_m is the absolute melting point of silver. Since the metallic bonds are believed to form on contact, since diffusion is not the cause of adhesion (ref. 2), and since the welding time is short (100 ms or less), the term solid-state resistance welding is a more appropriate term than is diffusion welding (ref. 1). Solid-state welding was judged to be achieved if microexamination of unetched joints up to 1000x revealed no unwelded areas. Subsequent microprobe examination showed that in the solid-state weld areas, only a small amount of interdiffusion had occurred between Ag and Cu.

An instant after solid-state welding occurred under the electrodes, a Ag - 40-atomic-percent-Cu eutectic composition formed at, or very near, the solid-state weld interface and became a liquid phase when the joint was heated to 779°C (fig. 6 and ref. 3). When the eutectic formed, it flowed by capillary action and brazed unwelded areas of the joint. The brazing action can continue with Ag-Cu alloys of varying composition as resistance heating increases the temperature of the melt well above the eutectic temperature. The complexity of the metallurgical situation is considerable. For example, when initially solid-state welded areas are heated above the Ag-Cu eutectic temperature, they become molten and thus part of the brazed area of the joint. Note in figure 4 that there are unwelded areas between the electrodes and towards the outside of the electrode footprints. The former area is believed to contain trapped air which, as will be shown later, can result in voids in braze metal or in a weld nugget.

At the N contact weld just discussed, less heating effect was observed than at a P contact weld where brazing occurred between the electrodes (not shown). However, insufficient data are available to demonstrate whether this effect correlates with the contact area welded or with other welding variables.

Schedule B Welds

The two weld cross sections in figure 7 show a considerable difference in microstructure for the same weld schedule. This variation is at least partly due to the fact that maximum heating occurs midway through the joint. The P contact weld cross section (fig. 7(a)), was taken 30 percent through the joint. It shows a braze joint in the electrode gap and under the inside of the electrode footprints. A line of small pores is present in the Ag-Cu braze metal. Solid state welding took place beyond the braze.

More heating is evident at the N contact cross section of figure 7(b), 40 percent through the joint. In this case all of the silver has been melted between the electrodes to form a fusion weld nugget. This nugget is a Ag-Cu alloy. A brazed region borders the nugget, and solid-state welding took place beyond the limits of the braze.

The small pores in the braze joint of figure 7(a) and the large pores in the fusion weld of figure 7(b) are believed to be air bubbles formed in the molten braze or weld metal (discussed previously regarding fig. 4). The localized trapped air effect is also believed to have produced the bulge in the copper interconnect between the electrodes (fig. 7(b)).

Schedule C Welds

In figure 8 two fusion welds are shown with brazes and solid-state welds towards the outside of the electrode footprints. The weld nugget at the N contact (30 percent through the joint) is a Ag-Cu alloy (fig. 8(a)). The 1- μm SiO_2 layer on the cell acted as a refractory material to contain the Ag-Cu melt and thus prevent the nugget from alloying with the silicon. The SiO_2 layer also inhibited solid-state diffusion and possible formation of the Ag-15.4 atomic percent silicon eutectic which melts at 830° C (ref. 3 and fig. 9). Although no cell cracking is evident in figure 8(a), fine cracks in the silicon cell were observed under another similar Ag-Cu weld nugget.

At the P contact weld (40 percent through the joint) (fig. 8(b)) no protective SiO_2 layer was present on the silicon cell. This weld is similar to the N contact weld except that the weld nugget here is a Ag-Cu-Si-Pd alloy. The lens-shaped crack, observed under the weld nugget in fig. 8(b) is typical for all cases where the silicon cell was melted. Several factors contribute to the cracking. First of all the silicon cell has essentially no ductility at room temperature. Thus, local thermal shock alone could produce cracking. Second, solidification shrinkage of the pancake-shaped weld nugget must produce some deformation, that is, dishing under the weld nugget. Third, residual stresses are produced when the weld nugget contracts on cooling from the solidification temperature to room temperature, with the maximum residual stress being limited to the yield strength of the Ag-Cu-Si-Pd alloy (refs. 4 and 5).

Electron Probe Microanalysis

Electron-probe, continuous-line traverses were run on all three metallurgical classes of welds between the copper interconnect and the silicon cell:

- (a) Solid-state weld between Ag and Cu
- (b) Ag-Cu braze joint
- (c) Two fusion weld nuggets; one Ag-Cu, the other Ag-Cu-Si-Pd

For each weldment examined, microprobe traces confirmed the presence of thin layers of titanium and palladium, which had been intentionally deposited on the contact surface of the Si cells during manufacturing. These titanium and palladium microprobe traces are not shown in the figures for purposes of clarity. No attempt was made to confirm the presence of aluminum at the P contacts.

The solid-state weld joint of figure 10 shows a small amount of Ag-Cu interdiffusion. Interdiffusion between silver and silicon was nil. The dark band (about 1 μm wide) between the silicon and silver and the increase in microprobe specimen current in this vicinity gave evidence of the SiO_2 layer on the cell at this and other N contact areas.

This Ag-Cu braze joint (fig. 11) is only about 2.5 μm wide. Because of equipment limitations, it could not be established that the braze metal was of the eutectic composition. But the microprobe trace does show significant alloying near the Ag-Cu interface. Interdiffusion between silver and silicon was nil. Since this is a P contact area, no SiO_2 layer was present.

A microprobe trace of a Ag-Cu fusion weld nugget containing large trapped voids is shown in figure 12. In this case the silver coating was com-

pletely melted and formed an alloy of about 50 Ag - 50 Cu (weight percent). The 1- μm SiO_2 refractory layer in the N contact area protected the cell. Thus, the molten weld metal nugget was prevented from alloying with the silicon solar cell.

The fusion weld nugget (fig. 11) is an alloy of Ag-Cu-Si and palladium. Although the quantity of palladium was very slight, the microprobe traverse showed alloying of palladium in the weld nugget. The melting and alloying of the silicon cell is evident by the wavy nugget/cell weld interface and by the microprobe trace. Since this was a P contact, there was no protective SiO_2 coating on the cell. Two cracks are shown in figure 13 in the silicon below the weld nugget. Lens-shaped cracking of this type occurred below the nugget in all cases where the silicon was melted, and thus became part of the weld.

CONCLUSIONS

1. Three metallurgical categories of resistance welds were identified under various conditions of parallel-gap resistance welding:

(a) Low heat for a long time: Combination solid-state welding and brazing under each electrode with an unwelded area between the electrodes.

(b) Moderate heat, intermediate time: A Ag-Cu braze joint between the electrodes with solid-state welding at the periphery.

(c) High heat for a short time: A conventional fusion weld nugget between the electrodes with brazing and solid-state welding at the periphery. This kind of weld is always accompanied by cracking in the Si cell if melting of the Si occurs.

2. The 1- μm layer of SiO_2 at the N contact areas of the cell proved to be a refractory barrier that contained the molten weld nugget and prevented interaction with the Si cell.

RECOMMENDATIONS

1. Programs to develop solar array welding technology should start with well-defined metallurgical goals.

2. The weld joint metallurgy required to give optimum solar-cell reliability should be identified.

3. The welding process, associated control systems, and NDE procedures should be tailored to give assurance that the metallurgical goals are achieved.

REFERENCES

1. Welding Terms and Definitions. American Welding Society, A3.0-80, 1980.
2. Ludemann, W. D.: A Fundamental Study of the Pressure Welding of Dissimilar Metals Through Oxide Layers. UCRL-50744, 1969.
3. Hansen, M.: Constitution of Binary Alloys. McGraw-Hill Book Co., Inc., 1958.
4. Linnert, G. E.: Welding Metallurgy. Vol. 2. American Welding Society, 1967.
5. Lancaster, J. F.: The Metallurgy of Welding, Brazing and Soldering. George Allen and Unwin Ltd., 1965.

TABLE 1. - PARALLEL-GAP RESISTANCE
WELDING SCHEDULES

[Electrode force, 8.9 N (2.0 lb); electrode pressure, 6.1×10^6 N/m² (885 psi); electrode gap, 0.30 mm.]

Schedule	Weld voltage, V	Weld time, ms (a)
A	0.58	100
B	.63	80
C	.68	50

^aApproximate

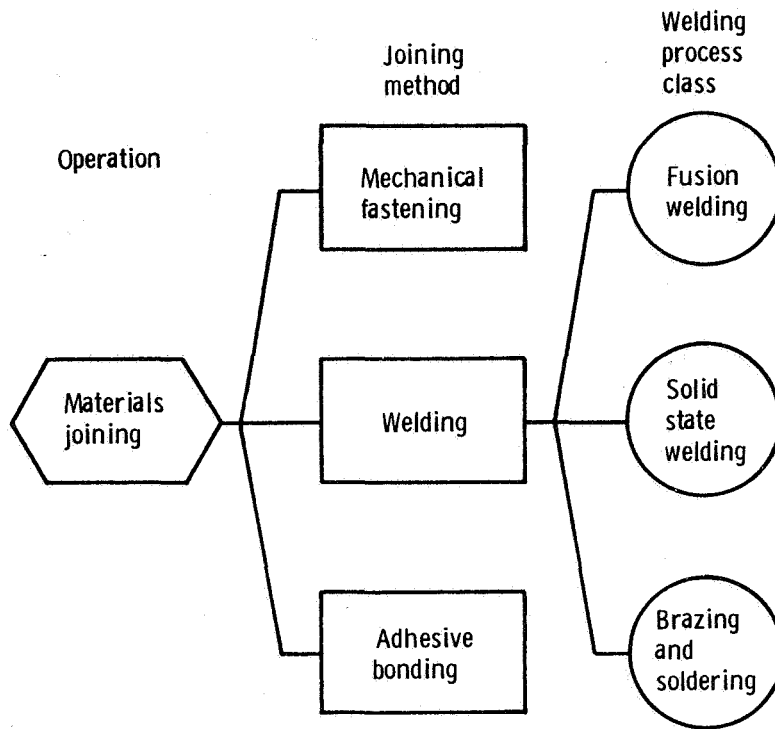


Figure 1. - Joining method diagram.

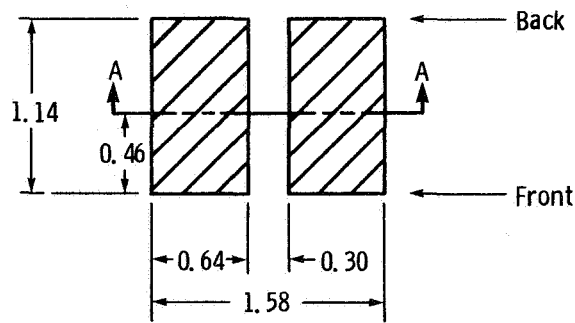


Figure 2. - Sectioning procedure.

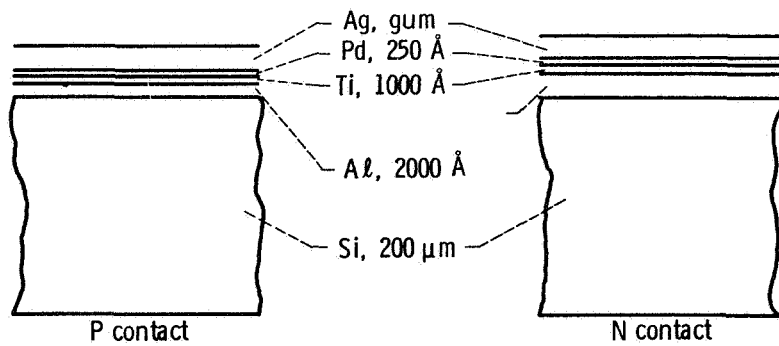


Figure 3. - Cell contacts.

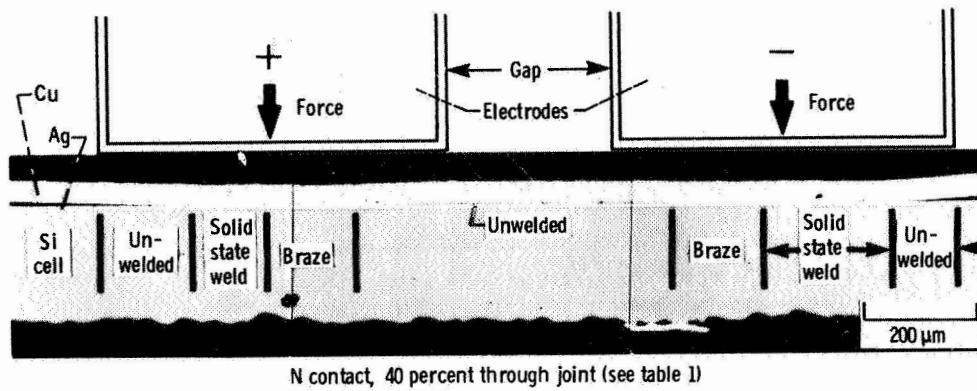


Figure 4. - Schedule A combination solid-state weld and braze joint. Air is believed to be in the unwelded area between the electrodes.

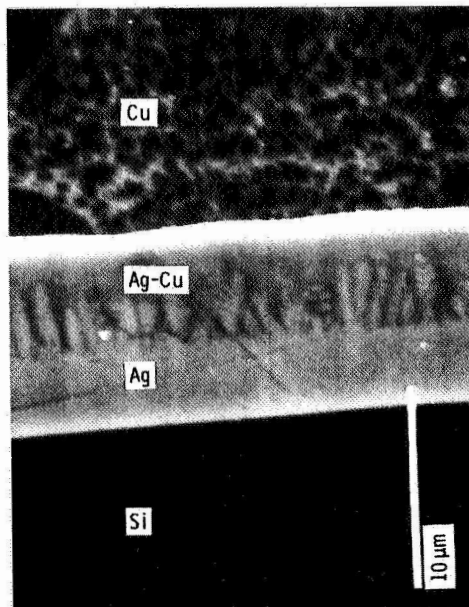


Figure 5. - Dendritic structure of an Ag-Cu braze metal in a schedule A weld at an N contact.

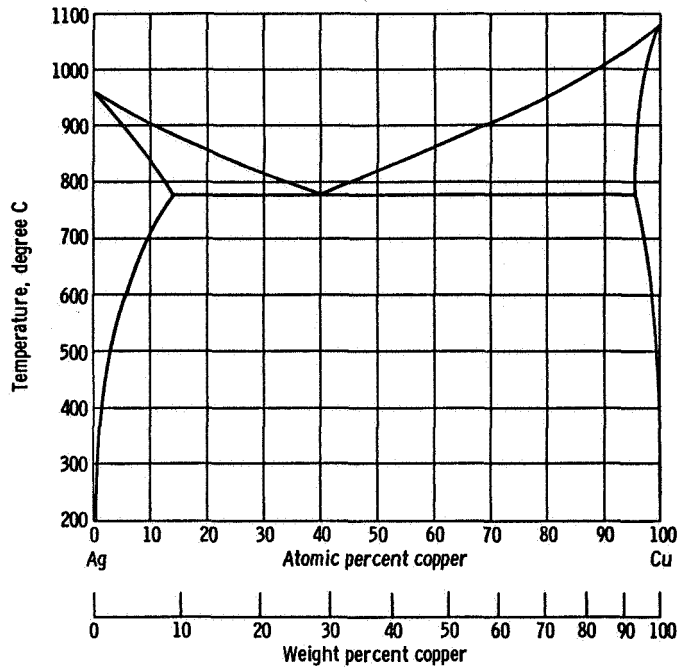
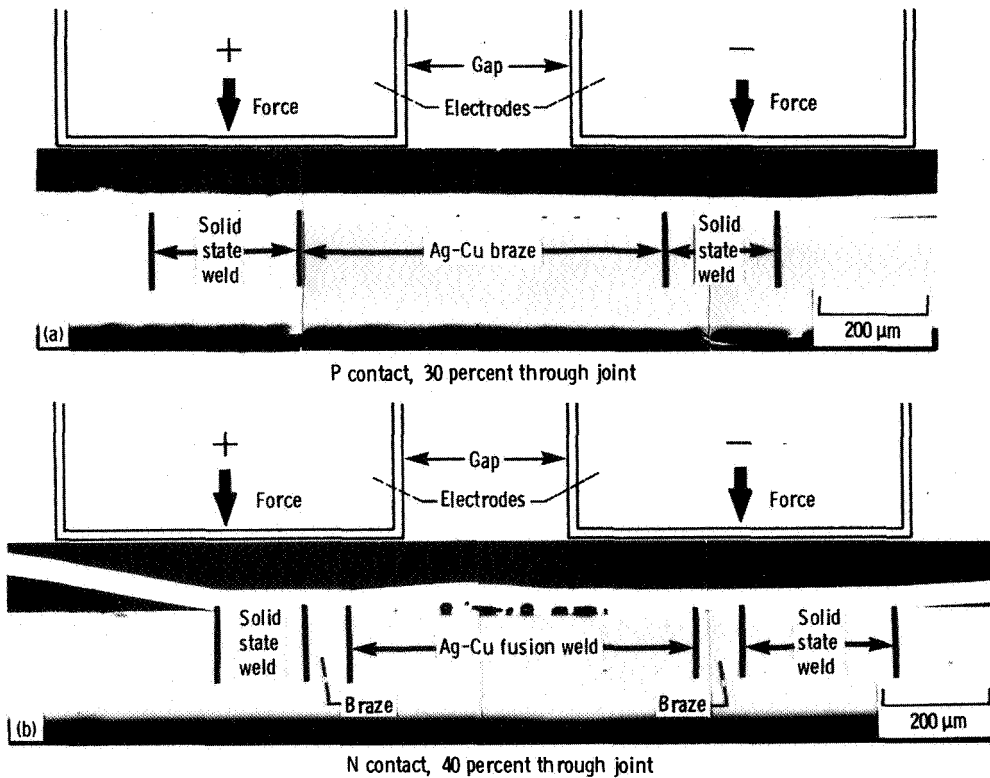
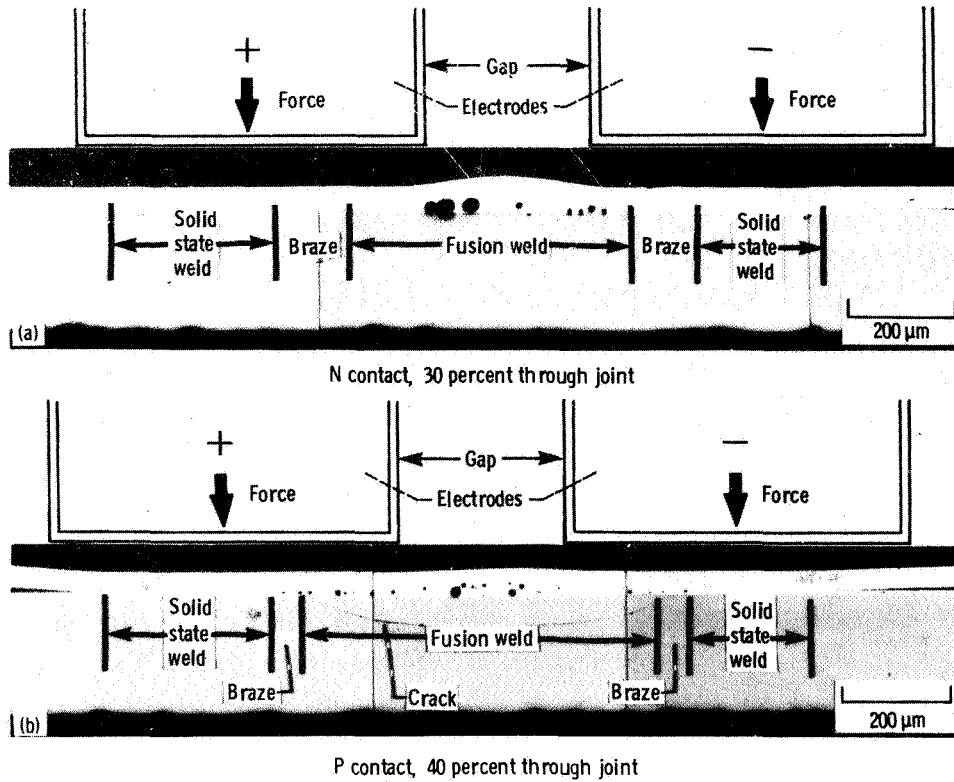


Figure 6. - Silver-copper equilibrium diagram (ref. 3).



- (a) Braze between electrodes with small voids in braze metal. Solid-state welds are outside of braze region.
- (b) Porous Ag-Cu fusion weld nugget producing bulge with brazing and solid-state welding outside of the nugget.

Figure 7. - Microstructural variations in schedule B welds.



- (a) Porous Ag-Cu fusion weld nugget with brazing and solid state welding outside nugget.
- (b) Porous Ag-Cu-Si-Pd fusion weld with brazing and solid state welding beyond the nugget. A lens-shaped crack in the silicon cell is present under the fusion weld.

Figure 8. - Microstructural variations in schedule C welds.

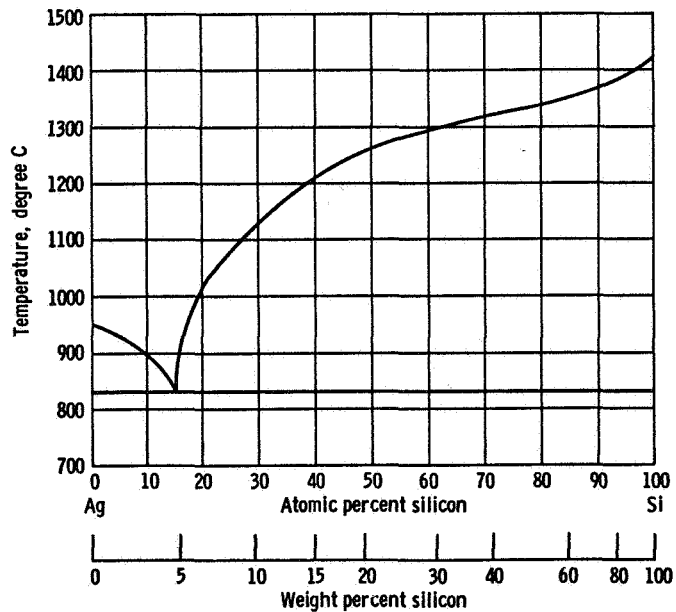


Figure 9. - Silver-silicon equilibrium diagram (ref. 3).

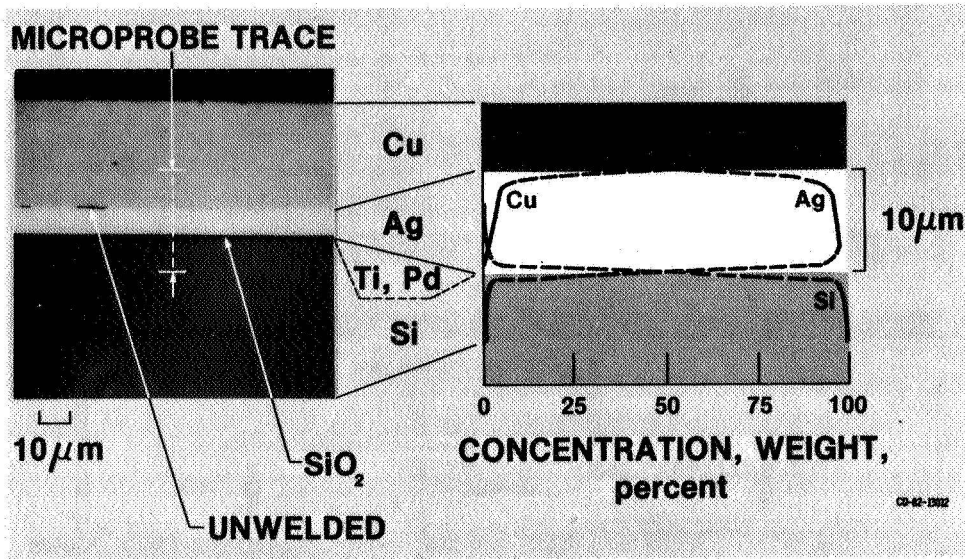


Figure 10. - Solid state weld at N contact area showing slight interdiffusion between silver and copper. Schedule C; weld under electrode.

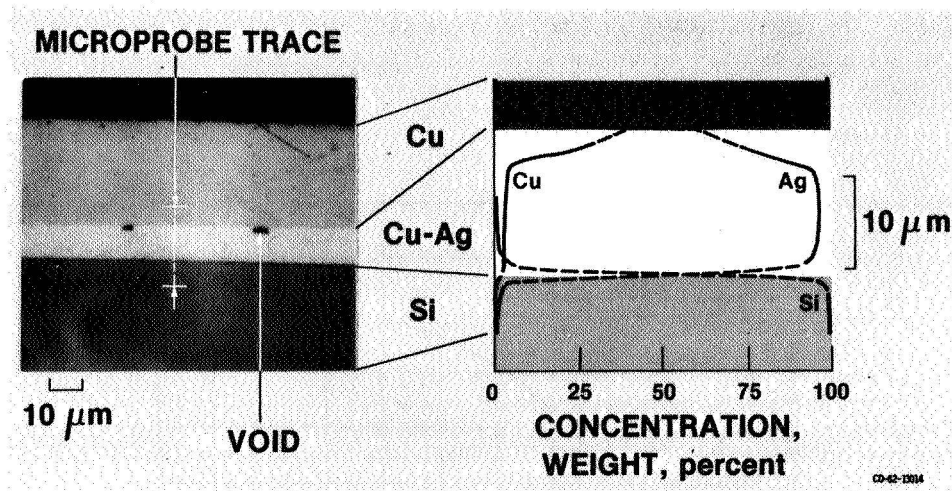


Figure 11. - Silver-copper braze joint, approximately 2.5 μm wide, with small voids in braze metal. Significant Ag-Cu alloying is shown at braze in this P contact joint.

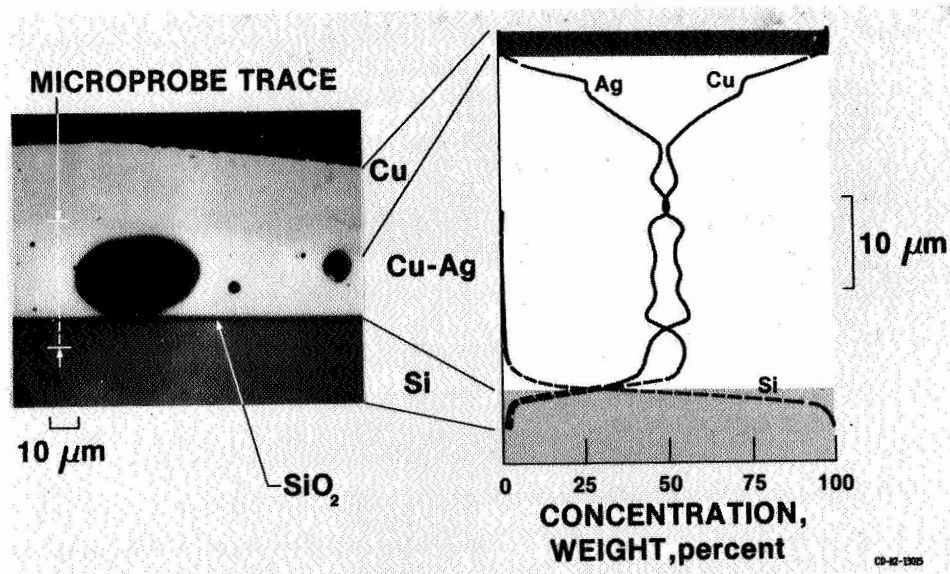


Figure 12. - Fusion weld nugget of Ag-Cu alloy at N contact with complete melting of silver layer. Schedule C; weld between the electrodes.

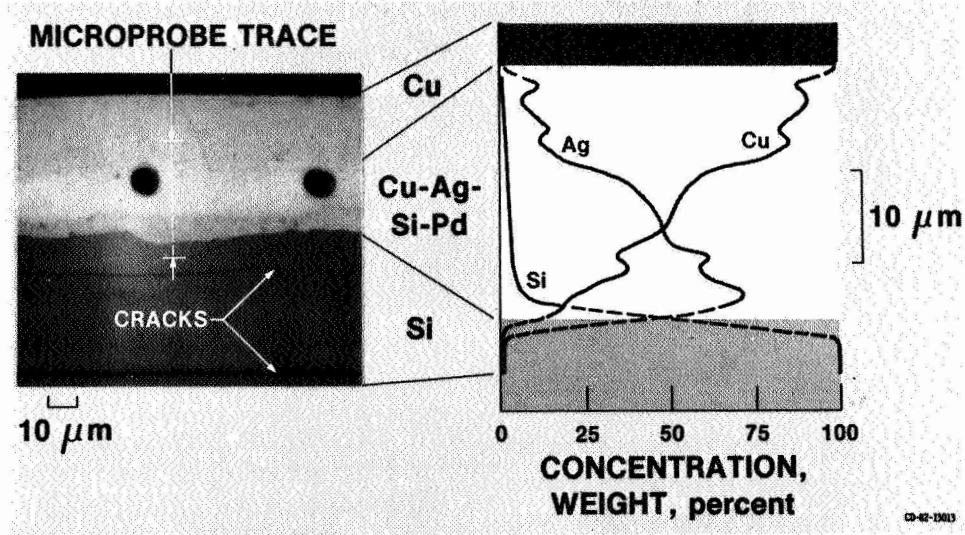


Figure 13. - Fusion weld nugget of Ag-Cu-Si-Pd alloy at P contact showing cracking in the silicon celllayer. Schedule C; weld between the electrodes.